JOURNAL OF CATALYSIS 92, 109–118 (1985)

Studies on Iron–Manganese Oxide Carbon Monoxide Catalysts

II. Carburization and Catalytic Activity

K. B. JENSEN[1] AND F. E. MASSOTH[2]

Department of Fuels Engineering, University of Utah, Salt Lake City, Utah 84112

Received February 28, 1984; revised October 26, 1984

Carburization studies of a series of reduced iron–manganese catalysts were done under synthesis gas (H_2/CO) conditions. Evidence was obtained for three types of carbon—carbidic, partially hydrogenated, and graphitic (coke-like carbon). These carbon types could be removed slowly with hydrogen; however, a relatively high temperature (500°C) was needed to remove all carbon. The low manganese oxide-containing catalysts showed greater specific activity for carbon monoxide and hexene hydrogenation than iron. The high manganese catalysts exhibited significantly increased hexene hydrogenation activity, possibly due to the presence of very small iron crystallites. Incorporation of manganese appears to chemically or electronically promote the active iron surface. In particular, it appears to alter the CO hydrogen reaction path by suppressing the direct formation of paraffins from the reactive intermediate, leading to higher olefins.

INTRODUCTION

Carburization is a word used to describe the surface and bulk property changes that occur to many Fischer–Tropsch catalysts during synthesis. Iron-based catalysts are well known to undergo carburization (*1*) and this fact must be considered in investigating their catalytic properties (*2*). In synthesis gas, the catalysts form iron carbides (*3, 4*) and carbonaceous material (*5–7*) and may also form iron oxides (*8, 9*). Iron carburization can occur at relatively moderate temperatures in carbon monoxide or H_2/CO mixtures. Usually, the final phase of the catalyst consists of either Hagg (χ) or hexagonal close-packed (ε) iron carbide (both have a stoichiometry of approximately Fe_2C). During the initial carburization, there has been some evidence, based on magnetization studies, for a transitory Fe_3C phase (*3*). The cementite phase (Fe_3C), however, is also a stable iron carbide that appears to be the principle carbide phase at temperatures greater than 500°C. But at lower temperatures, the Fe_2C carbides appear to be the preferred carbide phase (*10*).

We have previously characterized the reduced state of a series of iron–manganese catalysts (*11*), which had been used for carbon monoxide hydrogenation studies (*12*). The principle feature of the latter studies we address here is the variation in the olefin-to-paraffin ratio of the products with change in the manganese content of the catalyst.

EXPERIMENTAL

Catalysts were the same as those used previously (*11*). They consisted of a series of iron–manganese oxides; the number associated with each catalyst represents the approximate mole% Mn. The catalysts were generally activated by reduction in H_2 at 500°C overnight.

Catalyst carburization studies were carried out in a flow microbalance reactor. About 1/2 g of prereduced-passivated catalyst was heated in flowing H_2 at 500°C for 2 h before lowering the temperature. The

[1] Present address: Exxon Chemical Co., 4 Pearl Court, Allendale, N.J. 07401

[2] To whom inquiries should be addressed.

0021-9517/85 $3.00

weight gain due to carburization was then followed after introduction of a H_2/CO (synthesis gas) mixture, produced by flow monitoring of separate CO and H_2 streams. At an appropriate time, the mixture was replaced by H_2 and the ensuing weight loss followed. After weight line out, the temperature was raised to 500°C in H_2 to measure any additional weight loss. Carburized catalysts were characterized by XRD, PAS-IR, and TPR as described previously (*11*). In the latter case, the carburized catalyst ($2H_2/CO$, 250°C, 2 h) was cooled in the mixture to room temperature, followed by pure CO for 1/2 h; the catalyst was then flushed with H_2 and temperature programmed (10°C/min) in H_2.

The catalytic activities of reduced catalysts were performed in a flow microreactor at atmospheric pressure. The reactor consisted of a 1-cm-i.d. Pyrex tube. About 4 g of finely ground catalyst were held by a glass-wool plug, through which a thermocouple penetrated just into the bottom of the catalyst bed. After pretreating the reduced-passivated catalyst at 500°C for 1–2 h, the temperature was lowered to the described reaction temperature and the reactant introduced. For the CO hydrogenation tests, a 5% CO/H_2 mixture was used at a flow rate of about 100 cm^3/min. GC analysis for CO conversion was achieved with a carbo-sieve column and TC detector, the difference between the CO concentration in the reactor off gases and that from bypassing the reactor gave the CO conversion. For the 1-hexene hydrogenation tests, the hexene was introduced by passing H_2 (100 cm^3/min) through two hexene bubblers in series, the first at room temperature and the second at ice temperature. GC analysis was made with an *n*-octane on Porosil C column using an FI detector. Conversion was based on hexane produced. Carburized catalysts were also similarly tested. In this case, the catalysts were carburized in a H_2/CO mixture at 250°C prior to the test. Because of considerable differences in catalytic activity of the different catalysts, conversions varied from a few to up to 50%. Calculations revealed that mass transport should not have any effect on conversions under our reaction conditions.

Further details of these tests are given elsewhere (*13*).

RESULTS

Catalyst Carburization

A carburization and reduction cycle is shown for the pure iron catalyst in Fig. 1. Markers show the weight required for formation of Fe_3C and Fe_2C but do not necessarily indicate their formation. The weight changes involved were significantly larger than could be accounted for by carbon monoxide adsorption. Initially, the catalyst gained weight rapidly, then the weight gain slowed until a relatively slow but steady weight gain ensued.The change in rate occurred below the weight required for complete Hagg carbide formation (Fe_2C). Changing the reactant gas to pure hydrogen reversed the weight gain and approximately two-thirds of the weight gain was removed at 250°C. The catalyst returned to its initial weight after increasing the temperature to 500°C. Each step in this cycle required roughly 100 h for the pure iron catalyst.

Figure 2 shows two carburization–reduction cycles for an iron–manganese catalyst (C-15). The first cycle was performed at 250°C as with the pure iron catalyst. The initial carburization was somewhat slower than the pure iron catalyst and the second

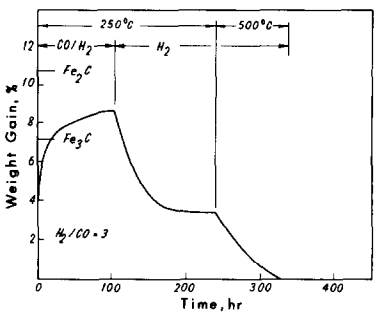

FIG. 1. Carburization and reduction weight profile for catalyst C-0.

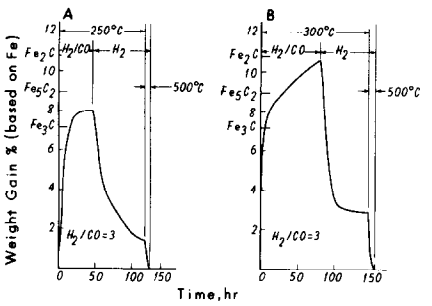

FIG. 2. Carburization and reduction weight profiles for catalyst C-15. (A) 250°C, (B) 300°C.

carburization region was also slower. The overall weight gain, on an iron basis, was similar for the two catalysts after about 40 h. The C-15 catalyst was only carburized for 40 h. Upon switching to H_2, the C-15 catalyst lost weight faster than the iron catalyst. Weight loss at 500°C was also significantly faster. The second carburization–reduction cycle, shown in Fig. 2B, was done at 300°C. The initial and second carburization rates were faster than at 250°C and more weight remained after hydrogen exposure at 300°C. Hydrogen reduction at 500°C proceeded quite rapidly. At both carburization temperatures, the weight removal rate in hydrogen was greater for the manganese-containing catalyst than for the pure iron.

Figure 3 shows the weight change data for the two catalysts during the initial phase of carburization and includes a lower temperature carburization run (225°C). At 300°C, the two catalysts appeared to carburize at about the same rate on an iron basis, but the rate of weight pickup was slower for the C-15 catalyst. At 225°C, the rate of carburization for C-15 was substantially slower than the C-0 catalyst and no evidence of a rate change with time was seen during this period.

Although not shown, the pure iron catalyst was allowed to carburize at 300°C for approximately 70 h, ultimately reaching a 12% weight gain. After 5 h, the weight gain was almost linear. After the run, the catalyst was examined by X-ray diffraction and evidence for Hagg carbide (χ-Fe_2C) was seen.

In order to compare results with catalysts run under processing conditions (*12*), several of the used catalysts from the latter runs were examined by XRD. The conditions of these tests were: 35 atm, H_2/CO = 2.0, space velocity of 1 cm^3/min · g, 210–240°C, CO conversions of 5–7%, on-steam time up to 12 h. Figure 4 shows that the principal phases were Fe and MnO, as was observed with the reduced catalysts (*11*). Peaks attributed to $MnFe_2O_4$ were not observed in these catalysts, although Maiti *et al.* (*14*) reported this phase in their used Mn–Fe catalysts. There is some evidence for other phases, probably Hagg carbide, but the lines did not exactly match any published pattern for iron and manganese oxide or carbide, and therefore some of the minor peaks remain unidentified. Although some

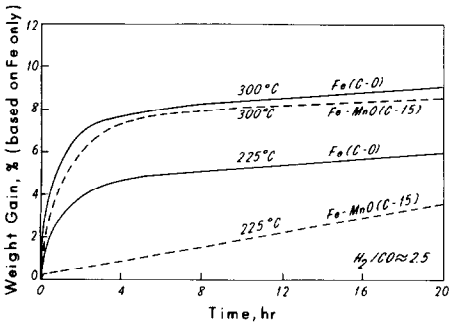

FIG. 3. Carburization weight profile comparisons normalized to weight iron basis.

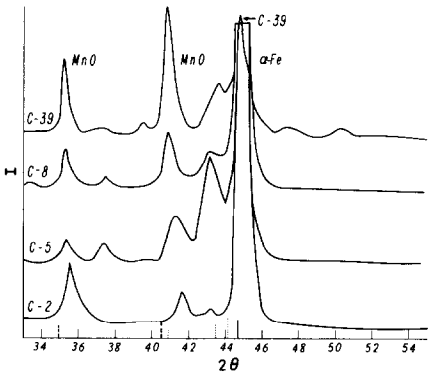

FIG. 4. XRD patterns of used iron–manganese catalysts. Markers: —, α-Fe; ---, MnO; ···, χ-Fe_5C_2.

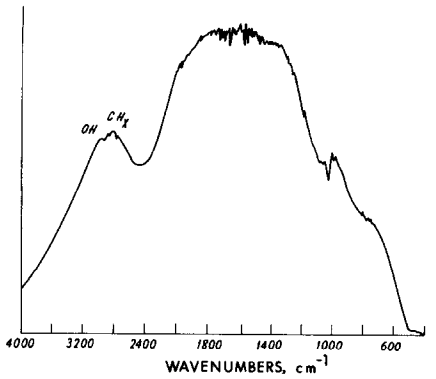

FIG. 5. Infrared photoacoustic spectrum of carburized catalyst C-3.

TABLE 1

TPR Results on Carburized Catalysts

Catalyst	Product			
	CH_4	H_2O	CO	CO_2
C-5	vl(400–500)	m(300–450)	vs(400–500)	Nil
C-15	vl(375–500)	s(450–500)	vs(25–150)	Nil
C-39	vl(340–500)	vs(350–450)	vs(70–120)	Nil
C-74	vl(400–500)	m(300–450)	s(80–150) s(350–450)	vs(350–450)
C-100	Nil	Nil	Nil	Nil

Note. Values in parentheses are temperature ranges in °C. Relative peak heights: vs, very small; s, small; m, moderate; vl, very large.

surface carbides are probably present, it is evident that extensive carburization of the catalysts had not taken place.

An ir photoacoustic spectrum of carburized catalyst C-3 is shown in Fig. 5. This catalyst had been carburized 3 h at 250°C in $2H_2/CO$ synthesis gas and then allowed to cool in synthesis gas. The ir photoacoustic spectrum revealed a large broad peak in the region 2500 to 3200 cm^{-1}. The reference spectra of the freshly reduced catalyst C-3 failed to show these peaks. This area of the ir adsorption spectrum can be attributed to hydroxy groups and carbon–hydrogen bonds. The broad peak is probably related to adsorbed hydrocarbons and other carbonaceous species formed during carburization. The erratic adsorption shown in the immediate right of 1800 cm^{-1} has usually been attributed to water.

Temperature-programmed reduction was carried out on a number of carburized catalysts on which CO had been adsorbed at room temperature. The results are summarized in Table 1. The temperature ranges of the main peaks are given in parentheses with their relative amounts. The significant feature of these results is the high evolution of methane for all the catalysts except pure MnO (C-100). Water evolution accompanied the methane, but at lower levels. Comparing these results with TPR of CO adsorbed on the reduced catalysts (Table 3 of Ref. (*11*)), the carburized catalyst produced significantly more methane while the amount of water liberated was not much different. Evolution of CO and CO_2 was low and similar to results on the reduced catalysts. From the results, it is obvious that the MnO catalyst neither carburized nor adsorbed CO to any measurable extent.

Catalytic Activity

1. Carbon monoxide hydrogenation. The results of CO conversion over several reduced catalysts are presented in Table 2. Rate constants were calculated from the

TABLE 2

CO Hydrogenation Activity of Catalysts

Catalyst	Fe surface area (m^2/g)	k_{CO}, μmole/g min (k'_{CO}, μmole/m^2 Fe min)	
		200°C	250°C
Reduced			
C-0	5.5	14.9(2.7)	38.8(7.1)
C-3	1.8	3.5(1.9)	12.0(6.7)
C-29	0.8	3.1(3.9)	11.4(14.2)
C-74	1.2	2.5(2.1)	6.3(5.2)
Carburized[a]			
C-0	5.5	14.5(2.6)	41.1(7.5)
C-3	1.8	3.4(1.9)	13.2(7.3)
C-29	0.8	1.7(2.1)	10.6(13.2)
C-74	1.2	2.7(2.2)	8.8(7.3)

[a] $2H_2/CO$ at 250°C for 3 h.

TABLE 3

Hexene Hydrogenation Activity of Catalysts

Reduced catalyst	Fe area (m^2/g)	k_H, cm^3/g min (k'_H, cm^3/m^2 Fe min) 100°C	150°C
C-0	5.5	Complete conversion	
C-5	1.7	Complete conversion	
C-74	1.2	20(17)	24(20)
C-100	0	Negligible conversion	

Carburized catalyst[a]	Fe area (m^2/g)	k_H, cm^3/g min (k'_H, cm^3/m^2 Fe min) 150°C	200°C	250°C
C-0	5.5	2.1(0.38)	6.2(1.13)	10.7(1.95)
C-5	1.7	0.7(0.42)	3.1(1.84)	5.7(3.4)
C-39	0.5	0.6(1.1)	3.3(6.6)	6.4(13)
C-74	1.2	2.5(2.1)	17.4(14.5)	—
C-100	0	0.1	0.1	0.1

[a] Carburized in $2H_2$/CO synthesis gas at 250°C for 3 h; these experiments were done in the presence of synthesis gas.

consumption of CO assuming zero order in CO (*15*). The upper section of the table gives the rate constants for the freshly reduced catalysts. The lower section of the table gives results for the same catalysts after carburization with $2H_2$/CO at 250°C for 3 h. The configuration of the catalyst bed (about 1 × 1 cm) was such that perfect plug flow was not assured. Therefore, the rate constants should be considered as approximate and their relative comparisons more valid than the absolute values. Although some CO consumption due to carburization could be expected with the reduced catalysts during reaction, this was apparently low enough under reaction conditions as not to significantly affect the results, since both rates and activation energies for the reduced and carburized catalysts were essentially the same. In general, the catalysts decreased in activity with increasing manganese content. For example, at 250°C, the addition of manganese was found to decrease the rate constant about one-third of its pure iron value for catalyst C-3. Further addition of manganese had a smaller effect on the rate constant. This trend was observed in both the freshly reduced and carburized catalysts.

Specific activities, based on iron surface area, are also listed for the freshly reduced and carburized catalysts. The iron surface area values were taken from the available carbon monoxide adsorption data reported earlier (*11*). The noticeable aspect of the data is that where previously the pure iron catalyst was most active on a weight basis, the manganese catalysts appear to have similar activities per unit iron surface.

2. Hexene hydrogenation. Hexene hydrogenation was used as a model reaction to investigate the olefin hydrogenation activity of the freshly reduced and carburized catalysts. Pseudo-first-order rate constants for the freshly reduced catalysts are shown in the upper portion of Table 3. The reduced iron catalyst was very active. Upon addition of manganese, a loss in activity per gram of catalyst was obtained, as well as a decrease in activity per unit iron area. Additional hydrogenolysis reactions occurred at the higher temperature, which resulted in a distorted temperature dependence of the calculated rate constants. The pure MnO catalyst was inactive for hexene hydrogenation. In the lower portion of Table 3, activities are given for hexene hydrogenation over carburized catalysts in the presence of synthesis gas ($2H_2$/CO). Synthesis gas was used in place of pure H_2 to obtain hydrogenation results under conditions more realistic of CO hydrogenation. On a weight basis, the presence of manganese lowered hydrogenation activity (except for C-74) and increased the activation energy. However, the manganese catalysts were found to have a higher specific activity for hydrogenation than pure iron. The manganese catalysts appeared to have a somewhat greater promotion for hydrogenation than carbon monoxide conversion, especially for the high manganese catalyst.

DISCUSSION

Catalyst Carburization

Carburization rates were studied on two

catalysts, the pure iron catalyst and an Fe–MnO catalyst containing 15 mole% Mn. With both catalysts, carburization showed two rate regimes, an initial, relatively fast regime, followed by a slow one. In many of the experiments, carburization was not evidently continued long enough to reach the expected fully carburized state; that is, the catalyst weight never reached the weight required to form stoichiometric Fe_2C. The overall rate of carburization of the Fe–MnO catalyst was considerably slower than the iron catalyst at 225°C but about the same at 300°C. During catalyst carburization, probably both iron carbides and carbonaceous material were forming, but their individual rate of formation could not be easily distinguished. The different carburization regimes and the different routes of carbon utilization complicate the caburization rate comparison between the two catalysts.

Bonzel and Krebs (*16*) found evidence for three types of carbon associated with carbon monoxide hydrogenation on iron: (1) a "carbidic" carbon, presumably related to surface iron carbide; (2) a partially hydrogenated carbon, CH_X; and (3) a "graphitic" carbon. Some direct and indirect evidence was also found for these types of carbon in the carburized iron–manganese catalysts.

Direct evidence for iron carbide formation was seen in the change of the X-ray diffraction patterns of the used catalysts after exposure to carbon monoxide and hydrogen at reaction temperatures. The appearance of peaks in the positions predicted for known iron carbides demonstrate that some carbidization occurred. The TPR results on the carburized catalysts showed that the greatest product evolved from hydrogen reaction of the carburized catalysts was methane, also a necessary condition for carbidization.

Evidence for the presence of a partially hydrogenated carbon specie comes from the ir spectrum of carburized catalyst C-3 (Fig. 5). The peak maximum occurs where C–H bond stretching frequencies are prevalent (*17*), and was not observed for CO adsorbed on the reduced catalyst (*11*). Another type of carbon associated with carburized iron catalysts, especially those carburized for long periods of time and at higher temperatures, is called "free" or "graphitic" carbon. Indirect evidence for this type of carbon was found with the extensively carburized catalysts C-0 and C-15. The presence of this type of carbon has often been determined by the temperature required for its removal with hydrogen (*18*). Podgurski *et al.* (*19*) claim that carbidic carbon can be quantitatively reduced at 300°C while removal of free carbon requires 500°C. More recently, Bonzel and Krebs (*16*) found that carbidic and partially hydrogenated carbon could be removed with hydrogen at 375°C, but graphitic carbon could not.

Catalyst Activity

1. CO hydrogenation. With freshly reduced iron catalysts, three basic processes are occurring during CO hydrogenation. A carbon balance on the system must include the formation of iron carbides and the buildup of the carbonaceous layer, as well as the formation of the expected gaseous products. Initially, the consumption of carbon by the iron can be important. In these experiments, after 2 or 3 h (Fig. 3), the rapid carbidization slowed down and the system approached closer to a steady-state condition. In related experiments, other investigators (*4*) have noted methane production to increase during the initial hour of reaction in synthesis gas with iron catalysts. The rate of formation of carbon deposits or carbonaceous layers appears to be relatively constant in the quasi-steady-state condition (*20, 21*) but its initial rate was difficult to estimate in these experiments. The reaction rate constants for iron catalysts, based on carbon monoxide consumption, before and after carburization, appear quite similar. Therefore, reaction over the reduced catalyst occurs very early on a car-

bon overlayer or carbide phase and subsequent carburization does not substantially change the active carbon surface layer. These results are in agreement with those of Matsumoto (*22*), who found that the extent of precarburization of a commercial iron catalyst did not affect its steady-state activity.

The effect of manganese on catalyst activity was not large. On a specific rate basis the manganese-containing catalysts were 1.5 to 2 times as active as pure iron; but on a weight basis, they were less than half as active. These results suggest that manganese oxide electronically or chemically alters the nature of the iron and carburized iron surface. Additional evidence for this comes from the lack of hydrogen adsorption (*11*), the greater apparent room-temperature dissociative adsorption of carbon monoxide (*11*) and the higher specific decarburization rates of the manganese-containing catalyst.

The effect of manganese on iron appears very similar to that of potassium, except for higher production of carbon dioxide in the latter case. Yang (*23*) showed that the hydrocarbon selectivity of potassium-promoted iron catalysts was similar to that produced by a manganese-promoted catalyst for a number of catalysts promoted with different amounts of potassium and manganese oxide. Methane and C_5 production were somewhat higher with the potassium-promoted catalysts; however, the olefin/paraffin ratios in the C_2–C_4 region were both approximately three. These results support the idea that manganese oxide can function like potassium oxide as an electron donor. However, the potassium-promoted catalysts facilitate the removal of oxygen via carbon dioxide. The mechanism for this removal has been ascribed to a water gas shift reaction (*1*). The water gas shift reaction appears not to be catalyzed by the manganese oxide promoter. Indeed, well-reduced ("green") manganese(II) oxide was found to be a poor catalyst for the water gas shift reaction (*24*). Since the activity of the iron surface produced by the two promoters appear to be similar, the water gas shift activity may be related to the promoters themselves.

2. Hexene hydrogenation. The object of these runs was to obtain separate evaluation of catalyst hydrogenation capability apart from the CO hydrogenation reaction. The first point to note is the high hydrogenation capacity of the reduced iron catalyst and the complete lack of hydrogenation of MnO (Table 3). Intermediate formulations gave lower specific hydrogenation rates which decreased with manganese content. Thus, the presence of MnO decreased the intrinsic hydrogenation activity of the iron phase present in the reduced catalysts.

The second and more important point is the strong deactivating effect due to carburization and/or the presence of CO on simple hydrogenation (Table 3). The effect of MnO is to decrease the hexene hydrogenation activity per gram of catalyst at low to moderate levels of Mn but to increase activity at high Mn levels. The lower activity at lower Mn levels is due to less effective Fe surface area available. However, the high activity at the high Mn level requires another explanation. We proposed that the latter catalyst consists of very small iron particles supported on MnO (*11*). These may exhibit different catalyst activity from larger particles. For example, small iron particles are known to have different magnetic, electronic, and catalytic properties (*25*). Also, less C_7 sites (iron atoms with seven neighbors) are available in small iron particles (*26*), and more step and kink sites would be present. They have also been shown to have different CO and H_2 adsorption behavior (*27*). Another possibility is the presence of strong metal–support interaction effects of the iron particles supported on the MnO phase leading to a difference in the metallic character of the iron (*28*).

In contrast to the reduced catalyst, the hydrogenation activity per unit Fe area of the carburized catalyst increased with in-

creasing MnO (except for pure MnO). Therefore, the hydrogenation activity is completely different for the reduced versus the carburized catalyst, and its role in CO hydrogenation must be assessed on the carburized catalyst. This situation did not occur for CO hydrogenation, where CO conversions were the same for reduced and carburized catalysts as discussed above.

3. Role of manganese. One of the goals of this research was to understand the role of manganese in altering the selectivity behavior of iron catalysts. The predominant phases present in the reduced catalysts are α-Fe and MnO (*11*). The Fe phase is very active for CO and hexene hydrogenation whereas the MnO phase has virtually no activity for these reactions. Since the effective Fe surface decreases sharply with small additions of Mn and then remains relatively constant over a large range, catalytic activity would be expected to follow this trend; and in fact, is found for both reactions on a weight basis. However, differences in intrinsic activity per unit Fe surface area are evident as discussed above, signifying that Fe surface area alone is not sufficient to define catalytic activity.

The effect of manganese on catalyst selectivities is more pronounced than on activities. For CO hydrogenation at 35 atm, Yang (*23*) and Tsai (*12*) found Mn to promote olefin formation for low and moderate promoted iron catalysts. With the same series of catalysts as investigated in the present study, it was found that the olefin/paraffin ratio increased with increasing Mn content up to about 40 mole% Mn and then decreased sharply at higher Mn contents (*12*). We will use the model compound reaction results obtained in the present study to explain these selectivity effects.

Ignoring oxygenated products (which are low) (12), the CO hydrogenation reaction can be viewed as a series of polymerization steps involving a hydrocarbon intermediate (I). The intermediate can propagate by addition of CH_2 or terminate by desorption as an olefin (O) or a paraffin (P). Consider the termination according to the scheme

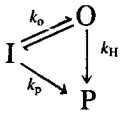

where k_o represents the overall rate constant for desorption as O, k_p for direct reaction to P, and k_H for hydrogenation of O in a secondary hydrogenation step via readsorption and hydrogenation (*29, 30*). After steady state has been reached, $k_o + k_p$ can be taken to be roughly equivalent to the overall CO hydrogenation rate constant, k_{CO}, while the hexene hydrogenation activity corresponds to k_H. Hence, the ratio of k_{CO}/k_H can be approximated by $(k_o + k_p)/k_H$. Values of this ratio from Tables 2 and 3 on a catalyst weight basis for the carburized catalysts are

	k_{CO}/k_H	
Catalyst	200°C	250°C
C-0	2.3	3.8
C-3, C-5	1.1	2.3
C-74	0.16	0.23

Here, we assume that catalysts C-3 and C-5, having compositions and properties close to each other, have identical activities. Since the k_{CO}/k_H ratio decreases with Mn content, $(k_o + k_p)/k_H$ decreases. For the low Mn-containing catalyst, $k_o + k_p$ (Table 2) decreases more than k_H (Table 3) relative to the Fe catalyst. Since the olefin-to-paraffin ratio could be expected to be approximately related to $(k_o - k_H)/(k_p + k_H)$, and this ratio *increased* with the low Mn catalyst, it follows that k_p must decrease appreciably more than k_o, i.e., MnO significantly decreases the direct formation path for paraffin formation. The increase in the k_{CO}/k_H ratio with temperature is also consistent with this conclusion, accounting for the general increase observed in the olefin/paraffin ratio with temperature (*12*).

For the high manganese content catalysts, the proposed presence of small iron particles (*11*) could dominate the selectivity behavior of these catalysts, which showed a significantly lower olefin/paraffin ratio (*12*). The much lower k_{CO}/k_H and larger k_H for catalyst C-74 signifies that now the greater hydrogenation activity is predominately responsible for the low olefin/paraffin ratio observed.

CONCLUSIONS

1. All of the iron-containing catalysts underwent carburization after exposure to synthesis gas. On an available iron surface area basis, the presence of manganese caused a lower carburization rate at 225°C, but the rate at 250°C was similar.

2. Evidence of three types of carbon was obtained for the carburized catalysts: a "carbidic" carbon, associated with the iron lattice; a partially hydrogenated carbon, associated with the active surface; and a "graphitic" or coke-like carbon, also present on or near the catalyst surface.

3. The iron- and manganese-containing catalysts used in the carburization studies could be decarburized with hydrogen. Lower temperature decarburization (300°C) apparently returned any formed iron carbides back to iron and removed the most active surface carbon. Higher temperatures (500°C) were needed to remove the rest of the carbon (presumably graphitic). The manganese oxide-containing catalyst decarburized more rapidly than the pure iron one. The removal rate of the graphitic or coke carbon in particular was faster with the manganese oxide-containing catalysts.

4. The manganese oxide-containing catalysts were somewhat less active than pure iron for carbon monoxide hydrogenation on a weight basis, but more active on a specific iron area basis. The freshly reduced and partially carburized catalysts were similar in carbon monoxide hydrogenation activity.

5. The hexene hydrogenation activity of the carburized catalyst mirrored their carbon monoxide hydrogenation activity for the low manganese content catalysts. However, for high manganese content catalysts, a significantly greater hexene hydrogenation activity was seen.

6. The high olefin-to-paraffin production of the low manganese catalysts during synthesis seems best explained as a chemical or electronic effect of the manganese oxide on the iron. This effect is similar to that observed with potassium, but without its carbon dioxide formation tendencies. Manganese oxide apparently lowers the rate of paraffin formation directly from an adsorbed intermediate.

7. The selectivity behavior of the high manganese catalysts in carbon monoxide hydrogenation, and their high hexene hydrogenation activity appeared best explained by small particle size effects, and perhaps manganese oxide–support interaction effects of the proposed small iron crystallites present in these catalysts.

ACKNOWLEDGMENTS

We thank Mr. J. A. Jiang of the Chemistry Department for the PAS-IR spectrum. This work was supported by the Department of Energy and the State of Utah.

REFERENCES

1. Storch, H. H., Golumbic, N., and Anderson, R. B., "The Fischer Tropsch and Related Synthesis." Wiley, New York, 1951.
2. Unmuth, E. E., Ph.D. dissertation, Northwestern University, Evanston, Ill. 1979.
3. Sancier, K. M., Isakson, W. E., and Wise, H., *in* "Hydrocarbon Synthesis from Carbon Monoxide and Hydrogen" (E. L. Kugler and F. W. Steffgen, Eds.), p. 178. Amer. Chem. Soc., Washington, D.C., 1979.
4. Stanfield, R. M., and Delgass, W. N., AIChE Natl. Mtg., New Orleans, November 1981, Preprint 9C.
5. Dwyer, D. J., and Somorjai, G. A., *J. Catal.* **52,** 291 (1978).
6. Bonzel, H. P., and Krebs, H. J., *Surf. Sci.* **91,** 499 (1980).
7. Ott, G. L., Ph.D. dissertation, Purdue University, West Lafayette, Ind., 1978.
8. Shultz, J. F., Seligman, B., Lecky, J., and Anderson, R. B., *J. Amer. Chem. Soc.* **74,** 637 (1952).
9. Shultz, J. F., Karn, F. S., Bayer, J., and Anderson, R. B., *J. Catal.* **2,** 200 (1963).

10. Browning, L. C., DeWitt, T. W., and Emmett, P. H., *J. Amer. Chem. Soc.* **72,** 4211 (1950).
11. Jensen, J. B., and Massoth, F. E., *J. Catal.* **92,** 98 (1985).
12. Tsai, Y. S., M. S. thesis, University of Utah, Salt Lake City, Utah, 1980; Tsai, Y. S., Oblad, A. G., and Hanson, F. V., *Amer. Chem. Soc., Fuels Div. Prepr.* **25**(2), 127 (1980).
13. Jensen, K. B., Ph.D. dissertation, University of Utah, Salt Lake City, Utah, 1980.
14. Maiti, G. C., Malessa, R., and Baerns, M., *Appl. Catal.* **5,** 151 (1983).
15. Dry, M. E., Shingles, T., and Boshoff, L. J., *J. Catal.* **25,** 99 (1972); Vannice, M. A., *J. Catal.* **37,** 449 (1975).
16. Bonzel, H. P., and Krebs, H. J., *Surf. Sci.* **109,** 1527 (1981).
17. Hair, M. L., "Infrared Spectroscopy in Surface Chemistry," Appendix A. Dekker, New York, 1967.
18. Walker, Jr., P. L., Rakszawaki, J. F., and Imperial, G. R., *J. Phys. Chem.* **63,** 133 (1959).
19. Podgurski, H. H., Kummer, J. T., and Emmett, P. H., *J. Amer. Chem. Soc.* **72,** 5382 (1950).
20. Dry, M. E., Shingles, T., and Botha, C. S. Van H., *J. Catal.* **17,** 341 (1970).
21. Dry, M. E., Shingles, T., Boshoff, L. J., and Botha, C. S. Van H., *J. Catal.* **17,** 347 (1970).
22. Matsumoto, H., *J. Catal.* **86,** 201 (1984).
23. Yang, C. H., Ph.D. dissertation, University of Utah, Salt Lake City, Utah, 1979.
24. Krupay, B. W., and Ross, R. A., *Canad. J. Chem.* **51,** 3520 (1973).
25. Storm, D. A., Ph.D. dissertation, Stanford University, Calif.
26. Dumesic, J. A., Topsøe, H., and Boudart, M., *J. Catal.* **37,** 513 (1975).
27. Topsøe, H., Topsøe, N., and Bohlbro, H. H., "Proceedings, 7th International Conference on Catalysis, Tokyo, 1980," p. 247. Elsevier, Amsterdam, 1981.
28. Tauster, S. J., Fung, S. C., and Garten, R. L., *J. Amer. Chem. Soc.* **100,** 170 (1978).
29. Schulz, H., Rosch, S., and Gokcebay, H., Symposium "Coal Phoenix of the 80's" at 64th Annual CIC Conf., Halifax, Canada, June 1981.
30. Novak, S., Madon, R. J., and Suhl, H., *J. Catal.* **77,** 141 (1982).